

# Effect of aqueous ozone treatment on the reduction of chlorpyrifos and physicochemical and microbial qualities of cucumber (*Cucumis sativus* L.): Process modeling and optimization

K. P. Navya<sup>1</sup> | K. P. Sudheer<sup>2</sup>  | S. Abdullah<sup>2</sup> | P. Vithu<sup>2</sup> | Berin Pathrose<sup>3</sup> | G. K. Rajesh<sup>1</sup>

<sup>1</sup>Department of Processing and Food Engineering, Kelappaji College of Agricultural Engineering, Kerala Agricultural University, Malappuram, India

<sup>2</sup>Agri Business Incubator, Department of Agricultural Engineering, Kerala Agricultural University, Thrissur, India

<sup>3</sup>Department of Agricultural Entomology, College of Agriculture, Thrissur, India

## Correspondence

K. P. Sudheer, Agri Business Incubator, Department of Agricultural Engineering, College of Agriculture, Vellanikara, Thrissur, India.

Email: [kp.sudheer@kau.in](mailto:kp.sudheer@kau.in)

## Abstract

A study was conducted at different combinations of ozone concentration (50%–100%) and time (10–30 min) to study the effect of aqueous ozone treatment on chlorpyrifos degradation in cucumber. A process was developed and compared using ANN-GA and RSM techniques. The optimum conditions obtained using RSM were ozone concentration of 95% and treatment time of 10 min. While the optimum conditions achieved by ANN-GA were ozone concentration of 81% and treatment time of 14 min. However, chlorpyrifos degradation is more at the condition optimized by ANN compared to the condition optimized by RSM. At the optimum condition, the cucumber showed superior physicochemical and microbial qualities, including pesticide degradation (91.08%), color change (3.58), firmness (11.75 N), moisture content (97.49%), water activity (0.93), pH (6.18), titratable acidity (0.06%), total soluble solids (2.1 °Brix), total plate count ( $1.5 \times 10^5$  CFU/g), and yeast/mold count ( $3 \times 10^5$  CFU/g), respectively.

## Practical applications

Increased awareness of the health benefits associated with the consumption of fruits and vegetables has led to a rise in their consumption. These items are primarily consumed in their raw or fresh state and often feature in salads. However, the presence of pesticide residues on the surface of raw fruits and vegetables can pose significant health risks to consumers. Ozone treatment can be used for effectively removing pesticide residue in the fresh-cut fruits and vegetables industry. Also, ozone treatment can reduce the microbial count on the surface of fruits and vegetables which enhances the shelf life of fruits and vegetables. Furthermore, it can prevent the natural ripening process of commodities, thereby increasing the consumer's acceptance. Ozone is considered a safe and eco-friendly alternative to chemical disinfectants and preservatives. It leaves no chemical residue on the produce and breaks down into oxygen, leaving no harmful byproducts, thereby ensuring safe consumption of the commodity.

## KEYWORDS

artificial neural network-genetic algorithm, ozonation, pesticide degradation, response surface methodology

## 1 | INTRODUCTION

Cucumber (*Cucumis sativus* L.) is an annual herbaceous climber fruit native to the tropical rainforest near the southern foot of the Himalayas. It has hairy leaves with 3–5 pointed lobes and is a delicate creeping vine. The fruits have a dark-green surface, crispy, moist-rich flesh, and little edible seeds concentrated at their core (Young, 2019). It is traditionally employed in various therapies and shows several medical features, including antibacterial activity, glycemic lowering ability, antioxidant capacity, and so on (Rolnik & Olas, 2020). Due to its flavor and texture, it is crucial as a fresh ingredient in salads as well as in processed foods like pickles and relishes (Ropelewska et al., 2022). However, the presence of residues of pesticides on the cucumber surface is creating a great threat to human health.

At present, pesticide application in vegetables has become increasingly frequent to control plant pests and thus reduce productivity losses (Oerke & Dehne, 2004; Ooraikul et al., 2011; Panuwet et al., 2012). One of the most popular groups of pesticides used in agricultural fields is organophosphates, and among all the organophosphates, chlorpyrifos stands out as the most popular due to its high efficiency and reasonable price (Harpicharnchai et al., 2013; Ooraikul et al., 2011; Pengphol et al., 2012). Nonetheless, organophosphates possess a high level of toxicity and result in the persistence of hazardous residues harmful to individuals, leading to health problems like impaired neuromuscular transmission and respiratory and cardiac issues (Chowdhury et al., 2012; Duangchinda et al., 2014; Ooraikul et al., 2011).

The use of chemicals like chlorine water and detergent is one of the easiest approaches for removing the pesticide residue. However, these substances are often restricted in the food sector and require approval as processing aids because of health concerns over the risk of chemical sanitizers. Another method for removing pesticide residues uses heat processes like sterilization and blanching. Although this technique is risk-free for health, it has a detrimental impact on the appearance, texture, and flavor of food products (Sánchez-Bravo et al., 2022). The use of ozone technology is considered a non-thermal food preservation technique that enhances food safety without lowering the quality or damaging the environment. The US Food and Drug Administration (FDA) designated ozone as generally recognized as safe (GRAS) in 1997 (Epelle et al., 2023). Also, ozone automatically decomposes into oxygen without leaving any hazardous leftovers in the food and the environment (Tiwari et al., 2008). In addition, unlike many thermal technologies, ozone conserves much energy as it is non-thermal and hence it does not require heat (Naik et al., 2022). The efficacy of ozone treatment in lowering chlorpyrifos contamination from vegetables has been reported in several studies (Chen, Hu, et al., 2020; Chen, Liu, et al., 2020; Sintuya et al., 2019).

However, a detailed study on the effect of ozone treatment on the reduction of chlorpyrifos in cucumber is not available in the literature. Therefore, this study aimed to optimize a process protocol for the reduction of chlorpyrifos contamination from cucumber without disrupting its quality, using ozone treatment. The detailed objective of this study is as follows: (a) to investigate the impact of ozone treatment on the reduction of chlorpyrifos and retention of quality of the

cucumber; (b) to examine the linear and combined effects of the independent parameters (ozone concentration and treatment time) on the quality of the cucumber; (c) to optimize the independent parameters for the maximum reduction of chlorpyrifos by employing and comparing response surface methodology (RSM) and artificial neural network (ANN).

## 2 | MATERIALS AND METHODS

### 2.1 | Raw materials

Fresh cucumbers with a maturity of 50–55 days from planting were procured from a farm close to Kerala Agricultural University, Vellanikara, Thrissur, Kerala. It was cleaned and sorted properly, then kept in a refrigerator until the ozone treatment.

### 2.2 | Chemicals

Chlorpyrifos (DURAMET TC<sup>®</sup> 20% EC) was purchased from FMC India Private Limited, Mumbai. The potato dextrose agar and plate count agar were purchased from Sisco Research Laboratories Pvt. Ltd., New Mumbai, India. All the other chemicals were purchased from Merck Life Science Private Limited, Mumbai.

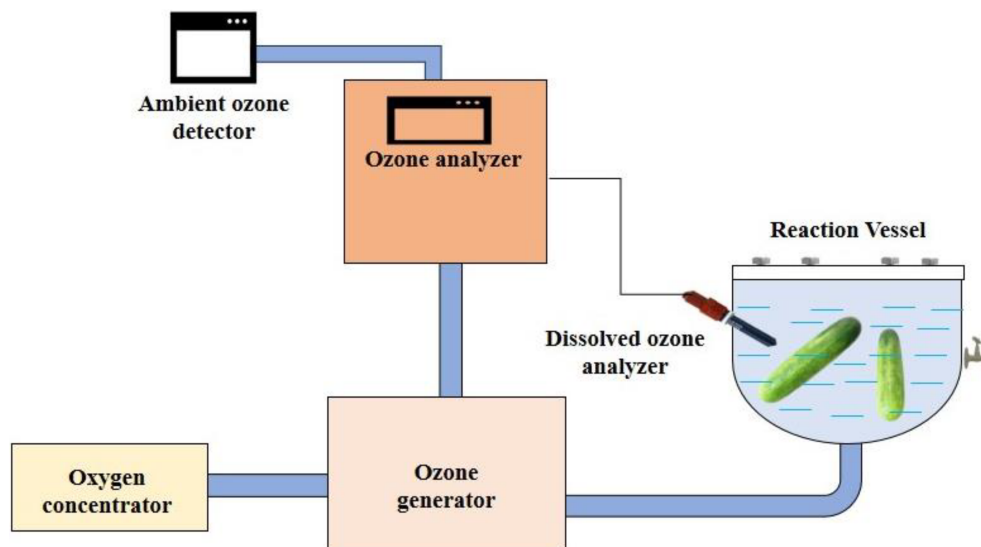
### 2.3 | Ozone treatment

The ozone processing experiment setup (Creative Oz-Air (I) Pvt Ltd, Uttar Pradesh, India) includes a reaction vessel, ozone generator, ozone gas destructor, oxygen concentrator, ozone analyzer, ozone dissolved monitor, and controller. The system uses ozone as feed gas with a nominal ozone concentration of 6%–10% wt.% (80–100 g/N m<sup>3</sup>) and a nominal feed pressure of 0.75–12 kg/cm<sup>2</sup>. Figure 1 shows the schematic representation of ozone equipment.

For all the treatments, 500 g of cucumbers were accurately weighed and dipped in the standard concentration (2.5 ppm) (CIBRC, 2020) of chlorpyrifos pesticide solution. Ozone was generated in the reaction tank of 5 L capacity that was filled with distilled water. The time of treatment and concentration of ozone were decided based on the experimental design. Immediately after ozone treatment, the cucumbers were subjected to different quality analyses. Similarly, the ozone-untreated pesticide-coated cucumber served as a control.

### 2.4 | Experimental design

The combination of independent parameters and the number of experiments for both the RSM and ANN were designed based on central composite design. In this study, there were 13 experiments with 2 factors (independent variables) and 5 central points. The

**FIGURE 1** Ozone setup in schematic form.**TABLE 1** List of independent variables with levels used in central composite design.

Independent variables	Units	Levels		
		-1	0	+1
Ozone concentration ( $X_1$ )	%	50	75	100
Treatment time ( $X_2$ )	min	10	20	30

software employed for the experimental design and statistical analysis was Design-Expert (version 12.0.3.0). Ozone concentration ( $X_1$ ) and treatment time ( $X_2$ ) were the independent variables, and pesticide degradation ( $Y_1$ ), color ( $Y_2$ ), and firmness ( $Y_3$ ) were the responses. The coded and real ranges of the independent variables (as shown in Table 1) were established after experimental trials.

## 2.5 | Analysis of quality attributes

### 2.5.1 | Sample preparation for chlorpyrifos residue analysis

Organic solvent (ethyl acetate) and salts ( $MgSO_4$  and  $NaCl$ ) were used to measure the chlorpyrifos residue from the cucumber samples, and clean-up sorbents were utilized for dispersive solid-phase extraction using the QuEChERS technique reported by Chanrattanayothin et al. (2020) with little modification. Initially, 10 mL ethyl acetate, 1 g sodium chloride, and 9 g anhydrous sodium sulfate were added to 10 g of ground cucumber. It was then homogenized at 14,000 rpm for 3 min followed by refrigerated centrifugation (Sorvall legend XTR, Thermo Fisher Scientific Inc, Langensfeld, Germany), at 3000 rpm for 5 min at 10°C. Later, 5 mL of the supernatant was transferred into 15-mL centrifuge tube having 250 mg primary secondary amine and 750 mg magnesium sulfate. After homogenizing the mixture, it was again centrifuged for 5 min at 5000 rpm and 2 mL of supernatant

was transferred into the vials after filtering through 0.2  $\mu m$  polytetrafluoroethylene membrane filter.

### 2.5.2 | Gas chromatography analysis for pesticide degradation

A gas chromatograph (Agilent 7890B) equipped with electron capture detector and HP-5ms capillary column with the particle size of 30 m  $\times$  250  $\mu m$   $\times$  0.25  $\mu m$  was used for pesticide residue determination. The carrier gas used was nitrogen (flow rate: 1 mL/min). Initial oven temperature was 80°C, it was then ramped to 180°C at 60°C/min and kept for 4 min, again to 213°C at 50°C/min for 0 min, to 214°C at 0.1°C/min for 0.3 min, to 240°C at 50°C/min for 0 min, to 240.5°C at 0.5°C/min for 0 min, and finally ramped to 300°C at 50°C/min and kept for 5 min, respectively. The pesticide residue was determined based on the peak area of the standard curve and the peak area of the sample. Finally, the pesticide degradation (%) was analyzed using Equation (1):

$$\text{Pesticide degradation (\%)} = \left[ \frac{\text{Initial amount of pesticide} - \text{Final amount of pesticide}}{\text{Initial amount of pesticide}} \right] \times 100. \quad (1)$$

### 2.5.3 | Determination of color

The outer peel of cucumbers alone was subjected to color measurement. Color indices were calculated according to the CIE  $L^*a^*b^*$  color space, using a Hunter lab colorimeter (MiniScan EZ, 4500L, USA). Under the CIE system, the color scale was expressed as  $a^*$  (redness and greenness),  $b^*$  (yellowness and blueness), and  $L^*$  (lightness). The luminance or brightness component,  $L^*$ , has a value between 0 and 100 (from black to white). The two chromatic components are the  $a^*$  and  $b^*$  values, which range from -120 to 120 (from green to red) and -120 to 120 (from blue to yellow), respectively (Carullo et al., 2022;

Sintuya et al., 2019). Finally, the color change following ozone treatment was determined using the equation explained by Gonçalves Ricci and Silva Costa Teixeira (2021).

## 2.5.4 | Firmness

Firmness of the sample was analyzed using EZ test, EZ-SX 500N (Shimadzu Analytical (India) Pvt. Ltd, Delhi) texture analyzer (probe: needle probe [2 mm diameter and 45 mm length]; test speed: 150 mm/min; test type: hardness test). The hardness test was performed in three replications and the values in Newton were taken from TRAPEZIUM X software.

## 2.6 | Other quality attributes

The following quality attributes were determined for the optimized samples.

### 2.6.1 | Moisture content and water activity

The estimation of moisture content of cucumbers was carried out by the standard AOAC procedure (AOAC, 2010). Similarly, the water activity of cucumbers was determined using a water activity meter (Aqualab, Decagon Devices Inc.; Pullman, WA, USA).

### 2.6.2 | Total soluble solids and pH

The total soluble solids (TSS) content of the samples was determined using the digital refractometer PCE-DR series (PCE Americas, Inc., USA). Similarly, the pH of the samples was determined using a digital pH meter ( $\mu\text{C}$  pH System 361, Systronics, India).

### 2.6.3 | Titratable acidity

In an Erlenmeyer flask, 1 mL of newly extracted cucumber juice was diluted to a final volume of 10 mL by adding distilled water, followed by two drops of phenolphthalein indicator. The mixture was then titrated against a 0.1 N NaOH solution until the pink color appeared. To obtain a concordant result, three iterations of the titration were performed. The amount of sodium hydroxide utilized was noted, and the titratable acidity was calculated using the equation explained by Joy and Anjana (2015).

### 2.6.4 | Total aerobic count and yeast/mold count

Initially, the necessary glassware and other equipment were thoroughly sterilized at 121°C for 15 min (Muniz et al., 2019) before

conducting the study. To begin with, the cucumber sample (10 g) was crushed and transferred into a beaker containing 90 mL sterile distilled water and was shaken well using a shaking incubator so that the surface microorganisms got into the water. Further, 1 mL of this mixture was taken and serially diluted from  $10^{-1}$  to  $10^{-5}$  and then 1 mL of each dilution was pour plated into the plate count agar for total aerobic bacteria and potato dextrose agar for yeast/mold taken in petri plates. Afterward, these plates were kept at 35°C for 48 h for aerobic bacteria and 25°C for 5 days for yeast and mold for incubation.

The microbial colonies on the plates were then counted using a digital colony counter (Infra Instruments Private Ltd., Chennai, Tamil Nadu), and the colony-forming units per gram of the treated sample were calculated using Equation (2):

$$\frac{\text{CFU}}{\text{g}} = \frac{\text{Mean number of colony – forming units} \times \text{dilution factor}}{\text{Volume of the sample}} \quad (2)$$

## 2.7 | Response surface methodology

RSM was used to develop the model and to optimize independent parameters to intensify the values of dependent parameters. In order to predict the optimal condition, the experimental data were evaluated using a second-order polynomial regression model (Equation 3), which is given by:

$$Y = a_0 + \sum_{i=1}^k a_i x_i + \sum_{j=1}^k a_{jj} x_j^2 + \sum_{j>i} a_{ij} x_i x_j \quad (3)$$

where Y represents the anticipated response values, with  $a_0$  and  $a_i$  denoting the coefficient for the linear term,  $a_{jj}$  for the quadratic term, and  $a_{ij}$  for quadratic interaction terms. Additionally,  $x_i$  and  $x_j$  signify the original values of the independent variables.

Design-Expert software (version: 12.0.3.0 State-Ease, Inc.) was used to develop experimental design, regression analysis, and graphical analysis and analysis of variance was used to analyze the significance of regression coefficients, validation of the developed regression model, statistical analysis, and the significant effect of independent variables. Moreover, numerical optimization of the Design-Expert software was utilized to optimize the independent variables to maximize the quality of the treated cucumbers.

## 2.8 | Artificial neural network

The experimental data were further subjected to ANN modeling with the help of the neural net fitting app from the MATLAB software (Version R2015a, The Math Works, Inc., Natick, MA, USA). The ANN model proposed for the ozone-treated cucumber consists of an input layer (representing the input variables: ozone concentration and treatment time), a hidden layer, and an output layer (representing responses) with 2, 10, and single neurons, respectively. Here, the

ANN model for each response was developed separately, hence the output layer comprised of single neurons. Additionally, the number of hidden layer neurons was 10, which was attained by the heuristic method with the least errors (maximum  $R^2$  and minimum MSE values) (Patra et al., 2022). Consequently, the design of the final ANN model is illustrated in Figure 2.

To facilitate the training of the data, the entire dataset was randomly partitioned into three subsets: 20% for testing, another 20% for validation, and the remaining portion for training purposes. The training process utilized the *trainlm* algorithm, which is based on the Levenberg–Marquardt back-propagation method. Likewise, the *tansig* (hyperbolic sigmoid) function and the *purelin* (linear) function were used as the transfer function for the hidden and output layers, respectively. Once the least MSE and maximum  $R^2$  were obtained, the training was stopped and the weights and bias values of the trained data were generated using the following equation (Equation 4).

$$Y_p = \text{purelin}\{W_o \times \text{tansig}(U_i \times X_i + T_h) + T_o\}, \quad (4)$$

where  $Y_p$  is the output (predicted) parameter;  $X_i$  is the input parameter;  $W_o$  is the weights between the output and hidden layer;  $U_i$  is the weights between input and hidden layer;  $T_h$  is the bias value of the hidden layer neurons; and  $T_o$  is the bias value of the output layer neurons (Patra et al., 2021a).

The independent variables of the developed models were further optimized using a genetic algorithm (genetic algorithm toolbox of MATLAB). The conditions for optimization were similar to the numerical optimization, mentioned above. However, the major parameters selected for GA optimization were selection function (roulette), crossover function (scattered), mutation function (adaptive feasibility), fitness scaling function (rank), creation function (feasible population), size (200), crossover fraction (0.8), and population type (double vector). All these functions were decided based on the study of Abdullah et al. (2022) and Manoj et al. (2023).

## 2.9 | Statistical analysis

All the experiments were conducted thrice and the values were expressed as mean  $\pm$  standard deviation. The efficacy of the constructed model utilizing both RSM and ANN were contrasted using statistical parameters like average absolute deviation (AAD), mean square error (MSE), mean percentage error (MPE), root mean square error (RSME), normal mean square error (NMSE), normal root mean square error (NRMSE), and coefficient of determination ( $R^2$ ) using the following equations (Equations 5–11). The model exhibiting the lowest MSE, AAD, MPE, NMSE, NRMSE, RMSE, and the highest  $R^2$  value is selected as the appropriate model for representing the responses.

$$\text{AAD} = \sum \frac{|X_{\text{pre}} - X_{\text{act}}|}{n}, \quad (5)$$

$$\text{MSE} = \sum \frac{(X_{\text{pre}} - X_{\text{act}})^2}{n}, \quad (6)$$

$$\text{NMSE} = \frac{\text{MSE}}{X_{\text{mean}}}; \quad (7)$$

$$\text{MPE} = \frac{100}{n} \sum \left| \left( \frac{X_{\text{pre}} - X_{\text{act}}}{X_{\text{pre}}} \right) \right|, \quad (8)$$

$$\text{RSME} = \sqrt{\frac{\sum (X_{\text{pre}} - X_{\text{act}})^2}{n}}, \quad (9)$$

$$\text{NRMSE} = \frac{\text{RMSE}}{X_{\text{mean}}}, \quad (10)$$

$$R^2 = 1 - \frac{\sum (X_{\text{pre}} - X_{\text{act}})^2}{\sum (X_{\text{pre}} - X_{\text{act}})^2}, \quad (11)$$

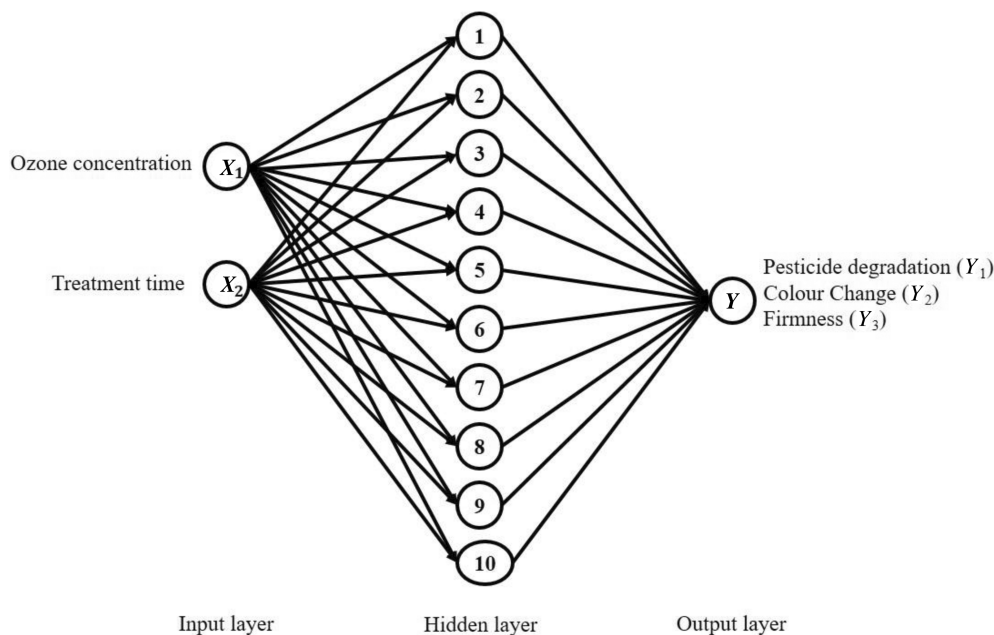


**FIGURE 2** The final design of the developed artificial neural network model.

**TABLE 2** Central composite design: experimental and predicted values of response at various experiment conditions.

Sl. No.	Ozone concentration (%)	Treatment time (min)	Pesticide degradation (%)			Color change			Firmness (N)		
			Exp. value	RSM pred value	ANN pred value	Exp. value	RSM pred value	ANN pred value	Exp. value	RSM pred value	ANN pred value
1	50	10	64.24 ± 0.1	64.36	64.24	7.14 ± 0.03	5.92	7.09	13.51 ± 0.2	13.22	13.25
2	100	10	87.16 ± 0.2	89.83	87.15	3.46 ± 0.02	2.99	2.14	11.46 ± 0.1	11.39	11.14
3	50	30	81.5 ± 0.1	78.41	83.69	8.41 ± 0.03	7.82	8.48	11.32 ± 0.2	11.2	11.32
4	100	30	89.18 ± 0.3	88.64	89.18	7.7 ± 0.02	7.87	7.32	10.43 ± 0.3	10.53	10.27
5	40	20	61.45 ± 0.2	63.46	65.59	2.91 ± 0.01	3.97	4.04	11.58 ± 0.1	11.83	11.66
6	110	20	90.30 ± 0.2	88.71	92.92	1.93 ± 0.03	1.93	2.19	10.12 ± 0.2	10.06	10.05
7	75	6	82.06 ± 0.1	79.99	82.06	5.98 ± 0.02	6.96	5.23	13.03 ± 0.3	13.24	12.96
8	75	34	86.6 ± 0.3	89.08	84.51	11.67 ± 0.01	11.75	12.59	11.22 ± 0.2	11.2	11.23
9	75	20	80.2 ± 0.2	82.12	82.73	7.54 ± 0.02	7.39	7.27	11.23 ± 0.1	11.75	11.69
10	75	20	85.4 ± 0.2	82.12	82.73	8.07 ± 0.03	7.39	7.27	11.94 ± 0.2	11.75	11.69
11	75	20	78.5 ± 0.1	82.12	82.73	6.87 ± 0.01	7.39	7.27	12.01 ± 0.2	11.75	11.69
12	75	20	82.2 ± 0.3	82.12	82.73	6.99 ± 0.02	7.39	7.27	12.02 ± 0.3	11.75	11.69
13	75	20	84.3 ± 0.2	82.12	82.73	7.49 ± 0.01	7.39	7.27	11.53 ± 0.1	11.75	11.69

Abbreviations: ANN, artificial neural network; RSM, response surface methodology.

where  $x_{pre}$  is the predicted value,  $x_{act}$  is the actual value,  $x_{mean}$  is the mean of experimental data, and  $n$  is the number of experiments.

### 3 | RESULTS AND DISCUSSION

#### 3.1 | Response surface methodology

##### 3.1.1 | Model fitting

The effect of two independent variables (ozone concentration and treatment time) on the three dependent parameters (pesticide degradation, color, and firmness) for ozone-treated cucumbers are provided in Table 2. Tables 3 and 4 display the regression coefficients as well as the AAD, MSE, MPE, RSME,  $R^2$ , Pred  $R^2$ , and Adj  $R^2$  for each second-order polynomial equation pertaining to ozone-treated cucumbers. The ANOVA findings for the three dependent variables in the created model demonstrate that models are acceptable with desired  $R^2$ , Adj  $R^2$ , and Pred  $R^2$ . According to Patra et al. (2021b), a constructed regression model should have an  $R^2$  value >0.8. Furthermore, the ideal model should have the lowest values of ancillary statistical indicators including MPE, AAD, MSE, and RSME. The models created here have minimum MPE, AAD, MSE, and RSME with an  $R^2$  >0.9 for each dependent parameter. In addition, there is an insignificant lack of fit for each dependent parameter. These outcomes demonstrated how appropriate the generated models were to the data.

##### 3.1.2 | Effect of ozone treatment on pesticide degradation

Cucumbers are mainly consumed in raw form or in the form of salads. But the problem with consuming it in raw form is that the pesticide

residues present on the surface of the product will lead to serious health problems in humans. Therefore, the pesticide residues from the products must be reduced with regard to consumer health. From Table 3, it is evident that the independent parameters such as ozone concentration ( $X_1$ ) ( $p < .001$ ) and treatment time ( $X_2$ ) ( $p < .001$ ) had a linear positive effect on ozone-treated cucumbers. Likewise, the interaction effect exhibited a notably positive impact in the context of  $X_1X_2$ , with a significance level of  $p < .05$ . Also, quadratic terms such as  $X_1^2$  ( $p < .05$ ) have a significant negative effect, and  $X_2^2$  ( $p > .05$ ) has a significant positive effect. Equation (12) encapsulates the regression model for pesticide degradation, with terms expressed in coded form:

$$\begin{aligned} \text{Pesticide degradation}(\%) = & 82.12 + 8.93X_1 + 3.22X_2 - 3.81X_1X_2 \\ & - 3.02X_1^2 + X_2^2. \end{aligned} \quad (12)$$

This equation yielded an  $R^2$  value of 0.9283, signifying that the regression model accounts for 92% of the variance in pesticide degradation for ozone-treated cucumbers. Figure 3a shows that pesticide degradation is positively correlated with an increase in both treatment time and ozone concentration. This could be explained by the oxidative potential of ozone gas which can break down the carbon chains and open the benzene rings in organic pesticides, disrupting unsaturated aliphatic moieties like alkynes and alkenes in their molecular structure. It also oxidizes functional groups like dichloro vinyl, nitro, methoxy, and amino as well as other functional groups. The molecular structure of organic pesticides is drastically altered by oxidative cleavage, which also renders them ineffective (Wang et al., 2019). A similar result was witnessed by Chen et al. (2013) when studied the effect of ozone concentration on pesticide degradation in Chinese white cabbage and green stem bok soy and the result was similar to Wu et al. (2007) while studying the effect of treatment time in *Brassica rapa*

**TABLE 3** Regression coefficient,  $R^2$ , Adj  $R^2$ , Pred  $R^2$ , and lack of fit of the responses.

Coefficients	Pesticide degradation	Color change	Firmness
$a_0$	82.12	7.39	11.75
$a_1$	8.93**	-0.72**	-0.63**
$a_2$	3.21**	1.70*	-0.72**
$a_{12}$	-3.81*	0.74	0.29
$a_{11}$	-3.02*	-2.22**	-0.40
$a_{22}$	1.21	0.98*	0.24
$R^2$	0.9283	0.9366	0.9285
Predicted $R^2$	0.6840	0.6132	0.7647
Adjusted $R^2$	0.8772	0.8913	0.8775
Lack of fit	Not significant	Not significant	Not significant

Note:  $a$  denotes the coefficient of the model equation;  $a_0$  denotes the constant terms; the linear effects are denoted by  $a_1$  and  $a_2$  (1 and 2 denote the ozone concentration and treatment time, respectively); interaction effect is denoted by  $a_{12}$  and quadratic terms are denoted by  $a_{11}$  and  $a_{22}$ .

\*Significant at  $p \leq .05$ .

\*\*Significant at  $p \leq .001$ .

**TABLE 4** Statistical analysis of responses.

	Pesticide degradation		Color change		Firmness	
	RSM	ANN	RSM	ANN	RSM	ANN
$R^2$	0.9283	0.9372	0.9366	0.9383	0.9285	0.9372
MSE	5.1780	5.1006	0.4365	0.3925	0.0556	0.0553
MPE	2.4307	2.2260	11.0465	9.1105	1.6815	1.6283
RSME	2.2755	2.258	0.6607	0.6265	0.2359	0.2352
NMSE	0.0639	0.0630	0.0659	0.0592	0.0048	0.0048
NRMSE	0.0281	0.0279	0.0997	0.0945	0.0203	0.0202
AAD	1.9734	1.7375	0.5272	0.4939	0.1985	0.1909

Abbreviations: AAD, average absolute deviation; ANN, artificial neural network; MPE, mean percentage error; MSE, mean square error; NMSE, normal mean square error; NRMSE, normal root mean square error; RSM, response surface methodology; RSME, root mean square error.

L. Hence, it has been observed that there exists a positive correlation between the degradation impact of ozone treatment on pesticide residue and the duration of treatment. Savi et al. (2015) reported that a similar trend was observed during pesticide degradation of wheat grain using gaseous ozone.

### 3.1.3 | Effect of ozone treatment on color change

As indicated in Table 3, the ozone concentration ( $X_1$ ) displayed a highly significant negative effect ( $p < .001$ ) on color, while treatment time ( $X_2$ ) exhibited a significant positive effect ( $p < .05$ ) on color. The interaction term between ozone concentration and treatment time ( $X_1X_2$ ) was nonsignificant ( $p > .05$ ), indicating that it does not have a significant effect on the color of ozone-treated cucumbers. Furthermore, the quadratic term of  $X_1^2$  ( $p < .001$ ) has a significant negative effect and  $X_2^2$  ( $p < .05$ ) has a significant positive effect. Equation 13 illustrates the regression model for color, with the terms expressed in coded form:

$$\text{Color change } (\Delta E) = 7.39 - 0.72X_1 + 1.69X_2 + X_1X_2 - 2.22X_1^2 + 0.98X_2^2 \quad (13)$$

The model possesses an  $R^2$  value of 0.9365, signifying its capacity to account for approximately 93% of the variability within the data. From Figure 3b, it is clear that initially an exponential increase was found in color value with an increase in concentration to 80% of ozone concentration. The maximum color value was obtained at a concentration of 80% ozone. Furthermore, the color value increases with treatment time and the maximum color value was obtained at a treatment time of 30 min. A similar result was obtained by Tiwari et al. (2009) in tomato juice, the color value was significantly reduced with an increase in concentration from 0% to 7.8% w/w and a treatment time of 10 min. Similarly, color degradation was also found in ozonated orange juice (Tiwari et al., 2008).

According to Tiwari et al. (2008), color degradation is due to the strong oxidizing effect of ozone that is derived from the nascent oxygen atom. There is limited research available regarding the

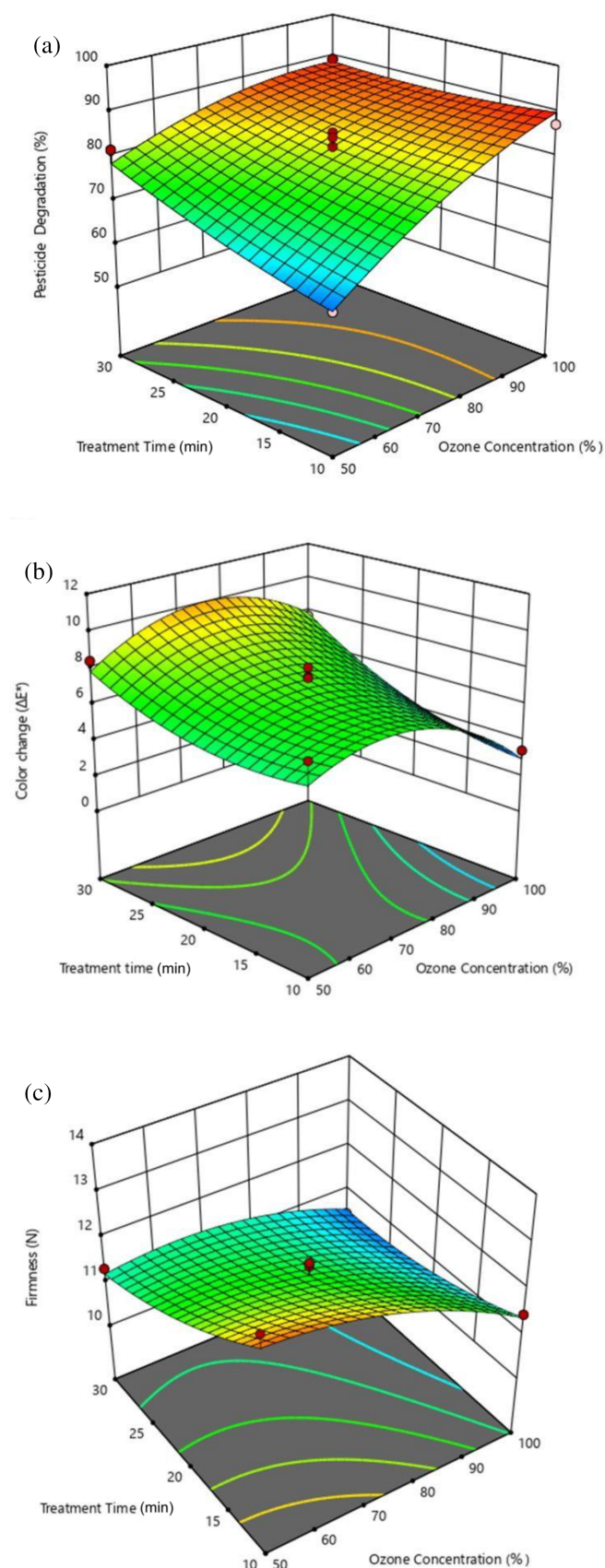


**FIGURE 3** Effect of ozone concentration and treatment time on pesticide degradation, color change, and firmness.

degradation of fruit juice color caused by ozone. To gain insights, one can draw comparisons with studies in non-food applications, particularly those involving synthetic and organic dyes.

### 3.1.4 | Effect of ozone treatment on firmness

Table 3 indicates that both ozone concentration ( $X_1$ ) ( $p < .001$ ) and treatment time ( $X_2$ ) ( $p < .001$ ) have a significant negative effect on firmness of ozone-treated cucumber. However, the interaction  $X_1X_2$  ( $p > .05$ ) does not show any significant effect on firmness of the sample. Whereas the quadratic terms  $X_1^2$  ( $p > .01$ ) and  $X_2^2$  ( $p > .05$ ) do not show any significant effect on the firmness of the sample. The subsequent equation depicts the influence of independent parameters on firmness, with the terms expressed in coded form:

$$\text{Firmness (N)} = 11.74 - 0.62X_1 - 0.72X_2 + X_1X_2 - X_1^2 + X_2^2. \quad (14)$$

The developed model showed an  $R^2$  value of 0.9285 which implies that it can explain 92% variability of data. From Figure 3c, it is clear that the firmness value slightly increases up to 75% ozone concentration, and later on, it starts to decrease slightly. It was also found that there is a slight decrease in firmness value with an increase in treatment time. Even though there is a slight decrease in the  $f_i$  value, the  $p$  value is significant ( $p < .001$ ). A similar result was demonstrated by Glowacz et al. (2015) in pepper. In the study, when pepper was exposed to  $0.3 \mu\text{mol mol}^{-1}$  concentration of ozone, a slight decrease in firmness was found but it was not significantly softer than the control sample.

## 3.2 | Numerical optimization

The optimum condition was selected based on the maximum value of desirability obtained for treatments. Here the optimum condition selected was 95% ozone concentration and a treatment time of 10 min with a desirability of 0.8. At this optimum condition, the predicted chlorpyrifos degradation was found to be 88.28%, color change of 4.14, and firmness of 11.74 N. The predicted values at optimum conditions were validated by conducting experiments under optimized conditions and it was found that there is no significant difference between the predicted value and the actual value.

## 3.3 | ANN modeling

### 3.3.1 | Model fitting

The *trainlm* algorithm, utilizing a criterion of minimizing MSE and maximizing  $R^2$  values, was employed in ANN to predict the pesticide degradation, color change, and firmness of the ozone-treated cucumbers.



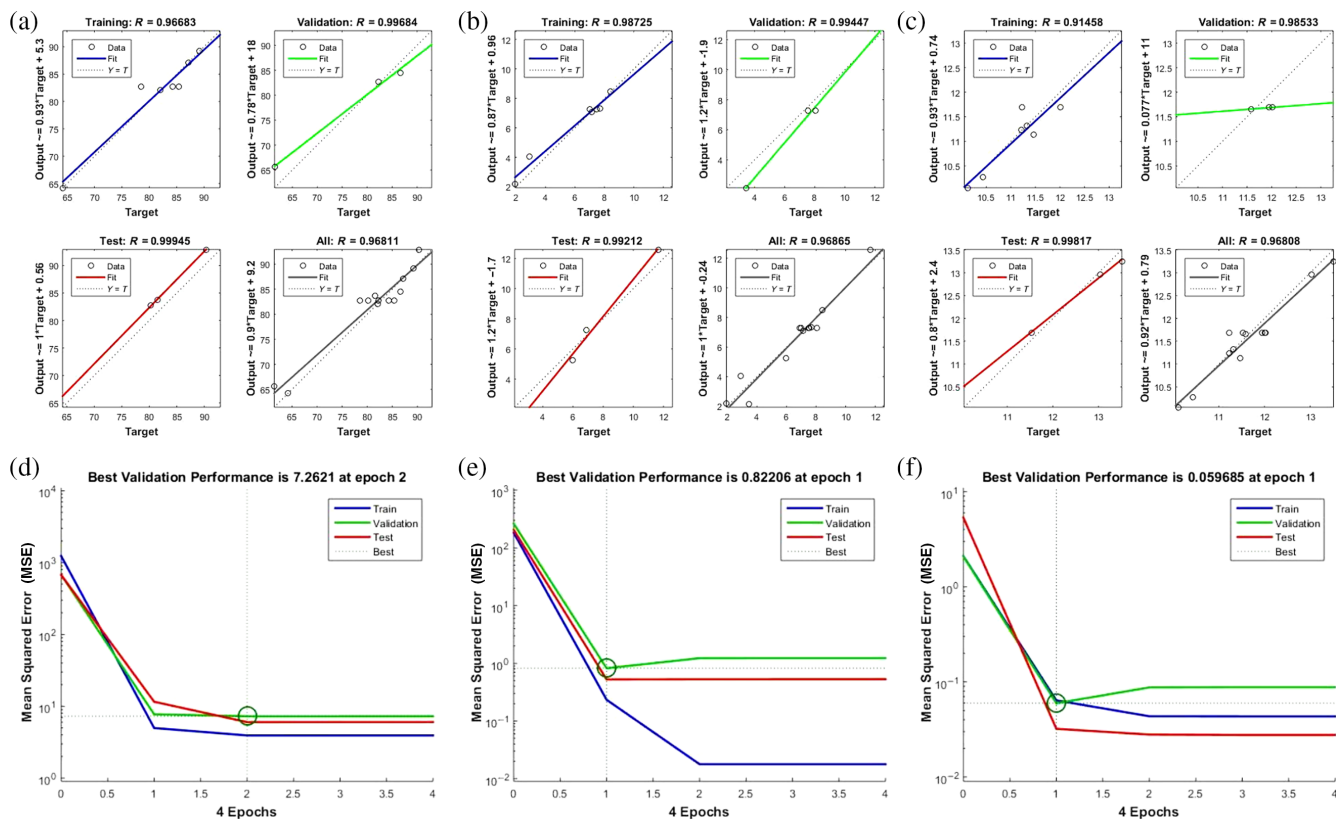


**FIGURE 4** The post-training regression and performance plot of pesticide degradation (a,d), color change (b,e), and firmness (c,f) of generated artificial neural network model.

The optimal model with the final framework is illustrated in Figure 2, which was achieved after four training epochs for all three response variables.

To ensure rigorous validation, the 13 experimental data runs were systematically segregated into three distinct sets. For pesticide degradation analysis, runs 1, 2, 4, 7, 10, 11, and 13 were allocated for training purposes, 5, 8, and 12 for validation, and 3, 6, and 9 for testing. The associated MSE values for training, testing, and validation were 3.9267, 6.0138, and 7.2621, while the corresponding  $R^2$  values were 0.9668, 0.9968, and 0.9995, respectively, as mentioned in Figure 4a,d. Likewise, as mentioned in Figure 4b,e, for the study of color change, runs 1, 3, 4, 5, 6, 12, and 13 were utilized for training, 2, 9, and 10 for validation, and 7, 8, and 11 for testing the model. The resulting MSE values were 0.2331, 0.8221, and 0.5255, accompanied by  $R^2$  values of 0.9873, 0.9921, and 0.9945 for training, testing, and validating the model, respectively. For the investigation of firmness, experimental runs 2, 3, 4, 6, 8, 9, and 11 were employed for training purposes, while 5, 10, and 12 were reserved for validation and 1, 7, and 13 for testing. The corresponding MSE values were calculated as 0.0640, 0.0597, and 0.0321, accompanied by  $R^2$  values of 0.9146, 0.9853, and 0.9982 for the training, validation, and testing segments, respectively, as mentioned in Figure 4c,f.

The effectiveness of the constructed ANN model in predicting unknown data is affirmed by the presence of the least MSE and higher  $R^2$  values. Model's performance and regression analysis are

illustrated in Figure 4. These figures elucidate the degree to which the experimental and predicted values align or fit together. This study has achieved overall  $R^2$  values of 0.9372, 0.9383, and 0.9372 and MSE values of 5.1006, 0.3925, and 0.0553 for pesticide degradation, color change, and firmness, respectively. This demonstrates a strong agreement between predicted and experimental value, affirming the solidity of the fitted model. Similarly, the bias and weight values for the constructed ANN models for all pesticide degradation, color change, and firmness are presented in the following matrices:

$$U_p = \begin{bmatrix} 4.4146 & -0.1133 \\ -0.0988 & 4.5319 \\ -2.8898 & 3.3562 \\ 4.1544 & 1.7134 \\ 3.4503 & -2.8049 \\ 1.5819 & -4.1196 \\ -0.8669 & 4.3231 \\ -3.7626 & -2.3213 \\ -4.4747 & 0.5418 \\ -0.6130 & -4.4124 \end{bmatrix}, \tag{15}$$

$$W_p = [0.4801 \ 0.1696 - 0.0351 - 0.2893 \ 0.5589 - 0.1513 \ 0.2924 - 0.3361 - 0.3319 - 0.2441], \tag{16}$$

$$TH_P = \begin{bmatrix} -4.4418 \\ 3.2884 \\ 2.4576 \\ -1.2951 \\ -0.5124 \\ 0.5064 \\ -1.5055 \\ -2.4720 \\ -3.3130 \\ -4.3667 \end{bmatrix}, \quad (17)$$

$$TO_P = [0.2646], \quad (18)$$

$$U_{\Delta E} = \begin{bmatrix} -3.9448 & -2.0548 \\ -0.7487 & 4.4196 \\ 1.8152 & 4.0253 \\ 4.1176 & -1.6641 \\ 0.7491 & 4.3643 \\ 4.1243 & -1.6643 \\ 3.4643 & -2.7475 \\ 1.9679 & 3.9673 \\ 4.2145 & 1.3256 \\ 4.0816 & 1.2878 \end{bmatrix}, \quad (19)$$

$$W_{\Delta E} = [-0.0784 \quad -0.0691 \quad 0.4959 \quad -0.4901 \quad -0.0888, \quad (20) \\ -0.4933 \quad 0.2095 \quad -0.1390 \quad 0.7240 \quad -0.1625]$$

$$TH_{\Delta E} = \begin{bmatrix} 4.4130 \\ 3.3489 \\ -2.4865 \\ -1.4296 \\ -0.4234 \\ 0.3511 \\ 1.3580 \\ 2.4558 \\ 3.4601 \\ 4.5493 \end{bmatrix}, \quad (21)$$

$$TO_{\Delta E} = [-0.1799], \quad (22)$$

$$U_F = \begin{bmatrix} -3.6565 & -2.3159 \\ 3.0581 & 3.1692 \\ 4.2421 & 0.2900 \\ 3.0562 & 3.2001 \\ 2.8229 & -3.4126 \\ -3.1833 & 3.0778 \\ -3.4925 & 2.7379 \\ 1.5704 & 4.1709 \\ -3.2947 & -2.9573 \\ -3.7941 & -2.2816 \end{bmatrix}, \quad (23)$$

$$W_F = [0.3433 \quad -0.1116 \quad -0.3109 \quad 0.0102 \quad -0.1753 \quad 0.0082, \quad (24) \\ -0.1835 \quad -0.4921 \quad 0.0299 \quad 0.0319]$$

$$TH_F = \begin{bmatrix} 4.5316 \\ -3.4684 \\ -2.6803 \\ -1.4791 \\ -0.3322 \\ -0.4054 \\ -1.3842 \\ 2.3982 \\ -3.4433 \\ -4.4269 \end{bmatrix}, \quad (25)$$

$$TO_F = [-0.4972], \quad (26)$$

where  $U$  is the connection weights between the input and hidden layers;  $W$  is the connection weights between the hidden and output layers;  $TH$  is the threshold value between the input layer and the hidden layer;  $TO$  is the threshold value between the hidden and outer layers. In addition, suffices P,  $\Delta E$ , and F represent pesticide degradation, color change, and firmness, respectively.

### 3.3.2 | GA optimization

The GA optimization process consists of a repetitive cycle of actions that include reproduction, crossover, and mutations, continuing until the least RMSE and MSE values between individual fitness and mean values were achieved. This condition was achieved after the 10th generation with a mean fitness value of  $-106.62$  (Figure 5). The optimal process conditions obtained at this best fitness point were 81% ozone concentration and 14 min treatment time. Also, 91.09% pesticide degradation, 3.58 color change, and 11.75 N firmness were the predicted responses at this optimum condition. Compared to numerical optimization, the predicted values were subsequently validated through experiments conducted under the identified optimal conditions. The findings affirmed that there was no substantial disparity between the actual and forecasted responses.

### 3.4 | Comparing RSM and ANN models

The forecasted outcomes from models created utilizing RSM and ANN were statistically compared using several metrics, including  $R^2$ , MSE, MPE, RSME, NSME, NRSME, and AAD. The results are summarized in Table 4. The statistical parameters all show that both models are quite predictable. However, ANN model has overall  $R^2$  values greater than the RSM model. Furthermore, the ANN model showed lowered values for MSE, MPE, RSME, NSME, NRSME, and AAD than the RSM model does. These results show that predictions made by the ANN model exhibit a significantly higher level of accuracy compared to those of the RSM model.

A study conducted by Patra et al. (2021a) compared both RSM and ANN for the isolation of phenolic compounds from bagasse of cashew apples using ultrasound. The results showed that all the statistical parameters resulted in a lower value for ANN compared to RSM and also showed a higher coefficient of determination ( $R^2$ ) for ANN which indicates that ANN modeling has good performance and accuracy. Similarly, result was also obtained by Patra et al. (2022) for the isolation of ascorbic acid, protein, and total antioxidants from bagasse of cashew apples using ultrasound. Furthermore, Jaddu et al. (2022) optimized kodo millets functional properties using RSM and ANN-GA. The results showed that ANN-GA was considered to be the optimal model for the optimization and modeling of kodo millet flour treated with cold plasma. Similar result was also obtained by Manoj et al. (2023) in valorization of fruit seeds by polyphenol recovery using microwave-assisted aqueous extraction.

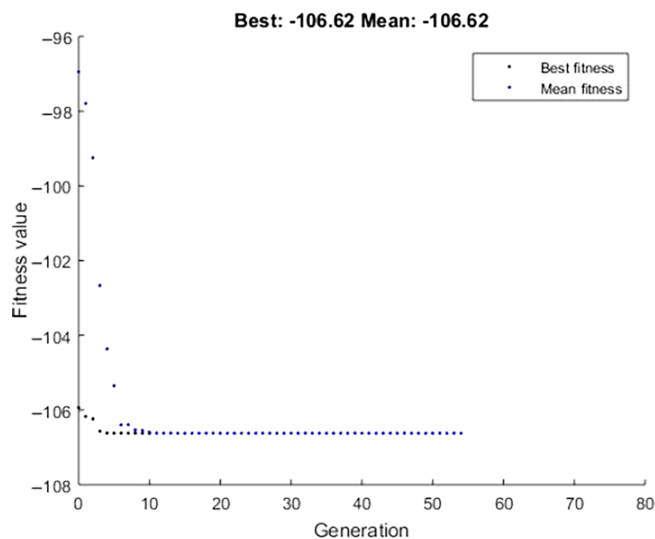


**FIGURE 5** The variations in fitness values across generations during the genetic algorithm optimization of ozone-treated cucumber.

**TABLE 5** Quality parameters of control (untreated) and chlorpyrifos-treated samples at RSM and ANN optimized conditions.

Properties	Control	RSM optimized	ANN optimized
Pesticide degradation (%)	-	88.21 ± 0.08	91.14 ± 0.09
Color change	-	4.15 ± 0.02	3.60 ± 0.04
Firmness (N)	11.74 ± 0.1	11.67 ± 0.10	11.76 ± 0.03
Moisture content (%)	96.53 ± 0.2	96.23 ± 0.13	97.5 ± 0.02
Water activity	0.93 ± 0.002	0.92 ± 0.01	0.95 ± 0.03
pH	6.19 ± 0.03	6.11 ± 0.03	6.2 ± 0.04
Titrateable acidity (%)	0.06 ± 0.002	0.05 ± 0.01	0.06 ± 0.02
TSS (°Brix)	2.13 ± 0.01	2.2 ± 0.03	2.1 ± 0.01
Total plate count (CFU/g × 10 <sup>5</sup> )	2 ± 0.02	2.6 ± 0.10	1.5 ± 0.10
Yeast/mold (CFU/g × 10 <sup>5</sup> )	3.2 ± 0.01	4.1 ± 0.10	3 ± 0.20

Abbreviations: ANN, artificial neural network; RSM, response surface methodology; TSS, total soluble solids.

### 3.5 | Quality of cucumber at optimum conditions

Various quality parameters of cucumber under RSM and ANN conditions and control sample are demonstrated in Table 5. From Table 5, it is clear that maximum pesticide degradation is obtained using ANN modeling compared to the RSM model. Also, the color change was minimal for the ANN optimized sample compared to RSM optimized sample. A  $1.5 \times 10^5$  CFU/g was obtained for total aerobic bacteria using the ANN model which was a significant reduction compared to the RSM model. Also, yeast/mold count was significantly reduced ( $3 \times 10^5$  CFU/g) using the ANN model. The reduction in microbial count is due to the antimicrobial properties of ozone (Brodowska et al., 2018) and oxidative potential of ozone leads to cell disruption of microorganisms.

Furthermore, the values of firmness, moisture content, water activity, pH, and titrateable acidity of ANN model and RSM model were in range with those of the control sample. This indicates that the process variables and the values showed no significant variations, indicating hardly any influence of ozone parameters.

## 4 | CONCLUSION

The effect of ozone treatment on chlorpyrifos degradation, firmness, and color of cucumber was analyzed, optimized, and predicted using RSM and ANN coupled with GA. The results of pesticide degradation, color change, and firmness were 88.28%, 4.14, and 11.74 N, respectively, for conditions optimized by RSM (ozone concentration of 95% and treatment time of 10 min). While the values of pesticide degradation, color change, and firmness were 91.08%, 3.58, and 11.75 N at conditions optimized by ANN (ozone concentration of 81% and treatment time of 14 min). The RSM and ANN models that were constructed both demonstrated high predictability. But with a higher  $R^2$  value and lower MSE, MPE, RSME, NSME, NRSME, and AAD values, it was discovered that the ANN model was superior to the RSM model. This shows ANN-GA modeling and optimization performed better and had higher accuracy than RSM modeling and optimization.

Moreover, chlorpyrifos degradation at the condition optimized by ANN was higher compared to the condition optimized by RSM. Also in ANN model, color change was minimal and firmness was within range with the control sample. The study comes to the conclusion that aqueous ozone treatment can be used as an ideal way to remove pesticide residue from cucumbers, as well as ANN-GA is a better method for modeling and process parameter optimization than RSM.

### CONFLICT OF INTEREST STATEMENT

The authors declare no conflicts of interest.

### DATA AVAILABILITY STATEMENT

The data that support the findings of this study are available from the corresponding author upon reasonable request.

### ORCID

K. P. Sudheer  <https://orcid.org/0000-0001-9981-2356>

### REFERENCES

- Abdullah, S., Karmakar, S., Pradhan, R. C., & Mishra, S. (2022). Pressure-driven crossflow microfiltration coupled with centrifugation for tannin reduction and clarification of cashew apple juice: Modeling of permeate flux decline and optimization of process parameters. *Journal of Food Processing & Preservation*, 46(6), e16497. <https://doi.org/10.1111/jfpp.16497>
- AOAC. (2010). *Official method of analysis. Association of official analytical chemists international* (18th ed.). AOAC International.
- Brodowska, A. J., Nowak, A., & Śmigielski, K. (2018). Ozone in the food industry: Principles of ozone treatment, mechanisms of action, and applications: An overview. *Critical Reviews in Food Science and Nutrition*, 58(13), 2176–2201.
- Carullo, D., Abera, B. D., Scognamiglio, M., Dons, F., Ferrari, G., & Pataro, G. (2022). Application of pulsed electric fields and high-pressure homogenization in biorefinery cascade of *C. vulgaris* microalgae. *Food*, 11(3), 471.
- Chanrattayanayothin, P., Peng-Ont, D., Masa-Ad, A., Warisson, T., Nirunsin, R., & Sintuya, H. (2020). Degradation of cypermethrin and dicofol pesticides residue in dried basil leave by gaseous ozone fumigation. *Ozone: Science & Engineering*, 42(5), 469–476.
- Chen, C., Liu, C., Jiang, A., Zhao, Q., Liu, S., & Hu, W. (2020). Effects of ozonated water on microbial growth, quality retention and pesticide residue removal of fresh-cut onions. *Ozone: Science & Engineering*, 42(5), 399–407.
- Chen, J. Y., Lin, Y. J., & Kuo, W. C. (2013). Pesticide residue removal from vegetables by ozonation. *Journal of Food Engineering*, 114(3), 404–411.
- Chen, L., Hu, C., Hood, M., Zhang, X., Zhang, L., Kan, J., & Du, J. (2020). A novel combination of vitamin C, curcumin and glycyrrhizic acid potentially regulates immune and inflammatory response associated with coronavirus infections: A perspective from system biology analysis. *Nutrients*, 12(4), 1–17. <https://doi.org/10.3390/nu12041193>
- Chowdhury, M. A. Z., Banik, S., Uddin, B., Moniruzzaman, M., Karim, N., & Gan, S. H. (2012). Organophosphorus and carbamate pesticide residues detected in water samples collected from paddy and vegetable fields of the Savar and Dhamrai Upazilas in Bangladesh. *International Journal of Environmental Research and Public Health*, 9(9), 3318–3329.
- CIBRC. (2020). *Major uses of pesticides: insecticides (up to 31 January 2020)*, Central Insecticide Board and Registration Committee, Directorate of Plant Protection, Quarantine and Storage. Retrieved from Department of Agriculture, Cooperation and Farmers Welfare, Ministry of Agriculture and farmers Welfare, Government of India website: [https://ppqs.gov.in/sites/default/files/approved\\_use\\_of\\_insecticides.pdf](https://ppqs.gov.in/sites/default/files/approved_use_of_insecticides.pdf)
- Duangchinda, A., Anurugsa, B., & Hungspreug, N. (2014). The use of organophosphate and carbamate pesticides on paddy fields and cholinesterase levels of farmers in Sam Chuk District, Suphan Buri Province, Thailand. *Science & Technology Asia*, 19(1), 39–51.
- Epelle, E. I., Macfarlane, A., Cusack, M., Burns, A., Okolie, J. A., Mackay, W., Rateb, M., & Yaseen, M. (2023). Ozone application in different industries: A review of recent developments. *Chemical Engineering Journal*, 454, 140188.
- Glowacz, M., Colgan, R., & Rees, D. (2015). Influence of continuous exposure to gaseous ozone on the quality of red bell peppers, cucumbers and zucchini. *Postharvest Biology and Technology*, 99, 1–8.
- Gonçalves Ricci, A. C., & Silva Costa Teixeira, A. C. (2021). Clarification of sugarcane juice by ozonation and anodic electrooxidation: Effects of process variables and energy consumption. *Sugar Tech*, 23(5), 1183–1191.
- Harnpicharnchai, K., Chaiear, N., & Chareerntanyarak, L. (2013). Residues of organophosphate pesticides used in vegetable cultivation in ambient air, surface water and soil in Bueng Niam subdistrict, Khon Kaen, Thailand. *The Southeast Asian Journal of Tropical Medicine and Public Health*, 44(6), 1088–1097.
- Jaddu, S., Abdullah, S., Dwivedi, M., & Pradhan, R. C. (2022). Optimization of functional properties of plasma treated kodo millet (open air multi-pin) using response surface methodology (RSM) and artificial neural network with genetic algorithm (ANN-GA). *Journal of Food Process Engineering*, 46, 1–12. <https://doi.org/10.1111/jfpe.14207>
- Joy, P. P., & Anjana, R. (2015). *Pineapple Research Station* (Kerala Agricultural University). Vazhakulam.
- Manoj, A. A., Fathima, A., Naushad, B., Sunilkumar, S., Shanker, M. A., & Abdullah, S. (2023). Valorization of fruit seeds by polyphenol recovery using microwave-assisted aqueous extraction: Modelling and optimization of process parameters. *Journal of Food Measurement and Characterization*, 17, 1–14.
- Muniz, C. R., Rosa, M. F., Andrade, F. K., Vieira, R. S., Morais, J. P. S., Nascimento, J. H. O., & Gama, F. M. P. (2019). Stable microfluidized bacterial cellulose suspension. *Cellulose*, 26(10), 5851.
- Naik, M., Sunil, C. K., Rawson, A., & Venkatachalapathy, N. (2022). Tender coconut water: A review on recent advances in processing and preservation. *Food Reviews International*, 38(6), 1215–1236.
- Oerke, E.-C., & Dehne, H.-W. (2004). Safeguarding production—Losses in major crops and the role of crop protection. *Crop Protection*, 23(4), 275–285.
- Ooraikul, S., Siri Wong, W., Siripattanakul, S., Chotpanarat, S., & Robson, M. (2011). Risk assessment of organophosphate pesticides for chili consumption from chili farm area, Ubon Ratchathani province, Thailand. *Journal of Health Research*, 25(3), 141–146.
- Panuwet, P., Siri Wong, W., Prapamontol, T., Ryan, P. B., Fiedler, N., Robson, M. G., & Barr, D. B. (2012). Agricultural pesticide management in Thailand: Status and population health risk. *Environmental Science & Policy*, 17, 72–81.
- Patra, A., Abdullah, S., & Pradhan, R. C. (2021a). Application of artificial neural network-genetic algorithm and response surface methodology for optimization of ultrasound-assisted extraction of phenolic compounds from cashew apple bagasse. *Journal of Food Process Engineering*, 44(10), e13828.
- Patra, A., Abdullah, S., & Pradhan, R. C. (2021b). Microwave-assisted extraction of bioactive compounds from cashew apple (*Anacardium occidentale* L.) bagasse: Modeling and optimization of the process using response surface methodology. *Journal of Food Measurement and Characterization*, 15(5), 4781–4793.
- Patra, A., Abdullah, S., & Pradhan, R. C. (2022). Optimization of ultrasound-assisted extraction of ascorbic acid, protein and total antioxidants from cashew apple bagasse using artificial neural network-genetic algorithm and response surface methodology. *Journal of Food Processing and Preservation*, 46(3), e16317.
- Pengphol, S., Uthaitutra, J., Arquero, O., Nomura, N., & Whangchai, K. (2012). Oxidative degradation and detoxification of chlorpyrifos by

- ultrasonic and ozone treatments. *Journal of Agricultural Science*, 4(8), 164.
- Rolnik, A., & Olas, B. (2020). Vegetables from the Cucurbitaceae family and their products: Positive effect on human health. *Nutrition*, 78, 110788.
- Ropelewska, E., Sabanci, K., & Aslan, M. F. (2022). Preservation effects evaluated using innovative models developed by machine learning on cucumber flesh. *European Food Research and Technology*, 248(7), 1929–1937.
- Sánchez-Bravo, P., Noguera-Artiaga, L., Gómez-López, V. M., Carbonell-Barrachina, Á. A., Gabaldón, J. A., & Pérez-López, A. J. (2022). Impact of non-thermal technologies on the quality of nuts: A review. *Foods*, 11(23), 3891.
- Savi, G. D., Piacentini, K. C., & Scussel, V. M. (2015). Reduction in residues of deltamethrin and fenitrothion on stored wheat grains by ozone gas. *Journal of Stored Products Research*, 61, 65–69.
- Sintuya, P., Narkprasom, K., Varith, J., Jaturonglumert, S., Whangchai, N., Peng-ont, D., & Nitatwichit, C. (2019). Degradation kinetics of diazinon and triazophos pesticides in dried chili under gaseous ozone fumigation. *Adapting to Challenges*, 27(S1), 169–178.
- Tiwari, B. K., Muthukumarappan, K., O'Donnell, C. P., & Cullen, P. J. (2008). Modelling colour degradation of orange juice by ozone treatment using response surface methodology. *Journal of Food Engineering*, 88(4), 553–560.
- Tiwari, B. K., O'Donnell, C. P., Brunton, N. P., & Cullen, P. J. (2009). Degradation kinetics of tomato juice quality parameters by ozonation. *International Journal of Food Science & Technology*, 44(6), 1199–1205.
- Wang, S., Wang, J., Wang, T., Li, C., & Wu, Z. (2019). Effects of ozone treatment on pesticide residues in food: A review. *International Journal of Food Science & Technology*, 54(2), 301–312.
- Wu, J., Schat, H., Sun, R., Koornneef, M., Wang, X., & Aarts, M. G. M. (2007). Characterization of natural variation for zinc, iron and manganese accumulation and zinc exposure response in Brassica rapa L. *Plant and Soil*, 291, 167–180.
- Young, D. (2019). *The backyard herbal apothecary: Effective medicinal remedies using commonly found herbs & plants*. Page Street Publishing.

**How to cite this article:** Navya, K. P., Sudheer, K. P., Abdullah, S., Vithu, P., Pathrose, B., & Rajesh, G. K. (2024). Effect of aqueous ozone treatment on the reduction of chlorpyrifos and physicochemical and microbial qualities of cucumber (*Cucumis sativus* L.): Process modeling and optimization. *Journal of Food Process Engineering*, 47(3), e14572. <https://doi.org/10.1111/jfpe.14572>